minerals

MDPI

Article

Strength Reduction of Coal Pillar after CO_2 Sequestration in Abandoned Coal Mines

Qiuhao Du [1,†], Xiaoli Liu [1,2,*,†], Enzhi Wang [1,2] and Sijing Wang [3]

1 State Key Laboratory of Hydro-Science and Engineering, Tsinghua University, Beijing 100084, China; duqiuhao1@163.com (Q.D.); nzwang@tsinghua.edu.cn (E.W.)
2 Sanjiangyuan Collaborative Innovation Center, Tsinghua University, Beijing 100084, China
3 Institute of Geology and Geophysics of the Chinese Academy of Sciences, Beijing 100029, China; wangsijing@126.com
* Correspondence: xiaoli.liu@tsinghua.edu.cn; Tel.: +86-10-6279-4910; Fax: +86-10-6278-2159
† These authors contributed equally to this work.

Academic Editors: Annalisa Martucci and Giuseppe Cruciani
Received: 3 November 2016; Accepted: 4 February 2017; Published: 17 February 2017

Abstract: CO_2 geosequestration is currently considered to be the most effective and economical method to dispose of artificial greenhouse gases. There are a large number of coal mines that will be scrapped, and some of them are located in deep formations in China. CO_2 storage in abandoned coal mines will be a potential option for greenhouse gas disposal. However, CO_2 trapping in deep coal pillars would induce swelling effects of coal matrix. Adsorption-induced swelling not only modifies the volume and permeability of coal mass, but also causes the basic physical and mechanical properties changing, such as elastic modulus and Poisson ratio. It eventually results in some reduction in pillar strength. Based on the fractional swelling as a function of time and different loading pressure steps, the relationship between volumetric stress and adsorption pressure increment is acquired. Eventually, this paper presents a theory model to analyze the pillar strength reduction after CO_2 adsorption. The model provides a method to quantitatively describe the interrelation of volumetric strain, swelling stress, and mechanical strength reduction after gas adsorption under the condition of step-by-step pressure loading and the non-Langmuir isothermal model. The model might have a significantly important implication for predicting the swelling stress and mechanical behaviors of coal pillars during CO_2 sequestration in abandoned coal mines.

Keywords: CO_2 sequestration; abandoned coal mine; adsorption; swelling effect; strength reduction

1. Introduction

Greenhouse gas emissions are the most important contributor to global climate change. Among all kinds of greenhouse gass, the contribution rate of CO_2 to greenhouse efficiency was 63% [1]. According to statistics, fossil fuel combustion and industrial emissions of CO_2 accounted for about 78% of total CO_2 emission in the ten years from 2000 to 2010 [2]. Currently, CO_2 storage in oil and gas fields, brine water, deep unmined coal seams and deep sea are considered to be effective and practical ways to reduce atmospheric CO_2 level, helping to slow global climate change and temperature rise trends, in the event that fossil fuels remain in use as a primary energy source. In the 2013 technology roadmap, the international energy agency (IEA) proposed an integrated approach to drop greenhouse gas emission by reducing the use of fossil fuels, improving energy efficiency, implementing new energy sources and carbon capture and sequestration (CCS) technology [3]. In addition, with the successful exploitation of coalbed methane and shale gas, its considerable economic benefit prompted many countries to begin in order to regard shale gas, coalbed methane, as alternative unconventional energy. Many scholars have proposed using CO_2 to enhanced coalbed methane (ECBM) production, and the

presence of CO_2 will mechanically weaken the coal and thus create fractures, helping to increase the permeability, improve the coalbed methane production yield and simultaneously sequestrate CO_2 [4–8]. In addition, for the residual space volume constituted by goaf areas and principle infrastructures in abandoned coal mines, some researchers proposed CO_2 sequestration in abandoned coal mines following the example of natural gas storage in it [9–12], which will be a potential option for CO_2 disposal because China has a large number of scrapped coal mines, and 541 key coal mines will be gradually closed by 2020. CO_2 can be stored in abandoned coal mines in three states: adsorbed on the remaining coal, free in empty space or dissolved in mine water.

The adsorption of CO_2 in coal can result in coal matrix swelling due to the fact that it has the highest adsorption potential compared with other fluids such as CH_4 and N_2. Currently, two mechanisms are applied to explain the adsorption-induced swelling in coal. On the one hand, several authors have widely researched the polymer structure, degree of cross-linking, three-dimensional polymeric network structures, as well as flexibility characteristics of coal macromolecules from the perspective of chemistry and molecules, and consider that the lower molecular-weight solvent, such as CO_2 and CH_4, can enter the macromolecule cross-linked polymer mesh, causing the coal matrix macromolecular structure rearrangement, resulting in swelling [13–17]. One the other hand, some scholars attribute the swelling being due to the formation of microfractures as the result of different pore systems, maceral components and mineral stiffness [18–21]. Hol et al. [22] considered CO_2 induced both reversible (i.e., adsorption-induced swelling and elastic compression) and irreversible (i.e., adsorption-induced microfracturing) strains under unconfined conditions.

Both ECBM and CO_2 sequestration in coal seams are concerned with the coal reservoir permeability behavior, the adsorption-induced swelling of coal matrix can compress the pore space and cleat system to result in the distinct decrease of the permeability of coal mass, and several models have been proposed from the consideration of effective stress, cleat volume compressibility, gas sorption-induced strain effect as well as pressure pulse decay [23–29]. Ranjith et al. [30] developed a triaxial equipment to study the gas fluid flow and found that coal mass permeability for CO_2 decreased largely with the increase of effective stress than that of N_2, due to the matrix swelling by CO_2 adsorption in coal. In addition, Verma and Sirvaiya [31] utilized the artificial neural network (ANN) to predict the Langmuir volume and pressure constants during CO_2 adsorption in coal, and that the ANN method was more accurate than other models in their study.

The effects of CO_2 adsorption on the strength of coal have been studied widely [32–34]. According to Gibbs' theory, when a more reactive, higher-chemical-energy adsorbate is used to displace the original adsorbate in solid adorbent, the surface energy of rock mass would reduce, which can lead to some reduction in initiation tension stress for fracturing and eventually the coal becomes more prone to damage. In addition, considering the thermodynamics of adsorption of gases in porous solids, the changes in surface energy at the interface between the gas adsorbate and solid adsorbent result in swelling through the conversion between surface free energy and elastic strain energy [35,36]. Based on the theory and experiment proposed by Meyers, a theoretical model was derived by Pan and Connell [37] through the energy balance approach. Hol et al. [38] developed a thermodynamic model based on statistical mechanics, and the model combined adsorption in a stress-supporting solid with the poroelastic to derive the relationship of stress–strain-sorption of coal under unconfined swelling condition. Liu et al. [39] revised the model derived by Hol et al. [38], and a corrected expression was obtained based on both statistical mechanics and kinetic approaches. Furthermore, Hol et al. [40] found the apparent bulk modulus determined for CO_2-equilibrated state was approximately 25% lower compared to the evacuated state through experiment data analysis. Ranjith et al. [32] studied the crack closure, crack initiation and crack damage of coal subjected to saturation with CO_2. Ranjith and Perera [41] considered the effects of the cheat system on strength reduction of coal after CO_2 adsorption. Perera et al. [42] experimented with adsorption of gaseous and super-critical CO_2 on bituminous coal from the Southern Sydney Basin, Australia, and studied the mechanical properties of coal sample before and after adsorption. The results showed that, compared with the natural state

uniaxial compressive strength (UCS), the gaseous CO_2 saturation reduced UCS by 53% and elastic modulus by 36% using gas saturation pressure of 6 MPa. However, the supercritical CO_2 saturation reduced UCS by 79% and elastic modulus by 74% using super-critical saturation pressure of 8 MPa. It is shown that the phase of CO_2 has a significant effect on physical properties of coal, the adsorption capacity, swelling effect and strength parameters.

Coal is a discontinuous structure comprised by many natural fractures and cleats (Figure 1), and coal seams are normally conceptualized by a matchstick model (Figure 2). After the colliery was scrapped, leaving pillars with a large number of cracks by mining action on both sides of the goaf. Meanwhile, CO_2 adsorption causes the coal mass to break down along the cleat system easily due to the fact that the adsorption mainly affects the cohesion of coal, and the reduction of cohesive force leads to the apparent plastic deformation areas. However, for the internal friction angle, it decreases to a certain extent and no longer keeps changes. Pillars with a large number of cleats and fractures act as sealing walls when CO_2 is stored in goafs and drifts. It means that the stability of the pillar decides the safety and sealing of CO_2 sequestration. Based on the above discussions and conclusions, it is significantly important to discuss the strength reduction of the coal pillar after CO_2 injection in the abandoned coal mines. In this paper, we focus our attention on strength reduction of the pillar when CO_2 sequestration in abandoned coal mines, through the relationship of sorption-strain based on unconfined conditions, and swelling-stress under uniaxial conditions. Finally, a strength reduction model is proposed to qualitatively understand the effects of CO_2 adsorption on the strength and failure mechanics of coal pillar in abandoned coal mines.

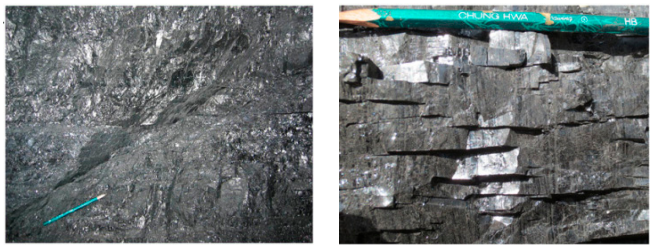

(**a**) (**b**)

Figure 1. (**a**) Fractures, Chengzhuang Mine (Reproduced with permission from [43]); (**b**) cleats, Chengzhuang Mine (Reproduced with permission from [44]).

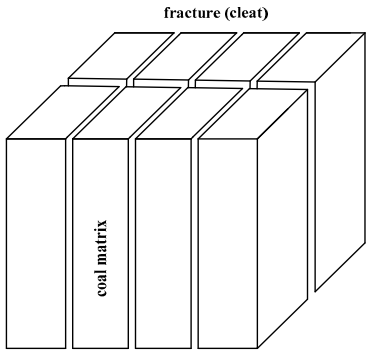

Figure 2. A matchstick model of a coal seam.

2. Theoretical Model

2.1. Adsorption-Induced Swelling Strain

CO_2 adsorption-induced volume strain has been studied by many researchers under unconfined conditions or uniaxial strain conditions [28,38,42]. In this section, we consider the adsorption-induced strain from the perspective of unconfined conditions. It is easy to measure the volumetric strain

value of test coal samples when carrying out a gas adsorption experiment in the laboratory under unconfined conditions. As shown in Figure 3, the sample is a cube with the side length l. Two lengths are measured as the base values for volume calculation. One located at parallel (l_{pa}) to its bedding plane, and the other is perpendicular (l_{pe}). The parallel and perpendicular displacements were Δl_{pa} and Δl_{pe}, respectively.

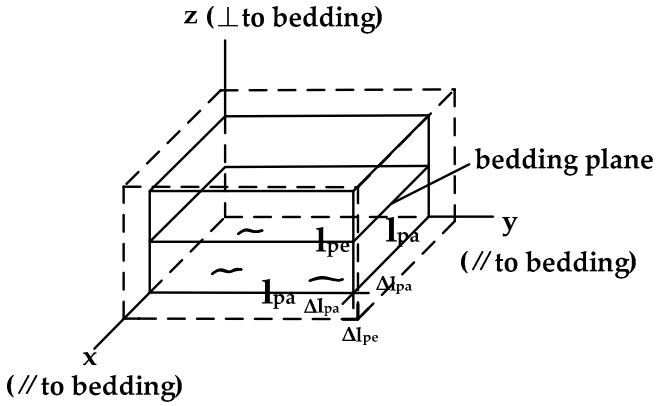

Figure 3. Sketch of original coal sample and swelling.

For the sake of convenience in the computation, it was assumed that parallel lengths and displacements of each block were equal and the perpendicular lengths and displacements were also equal. In this paper, the hypothesis that the coal mass satisfies the characteristics of isotropic and homogeneous is assumed. The reference value of volume was measured at the vacuum (initial volume V_0), and the volume increment was calculated based on the reference value with the pressure increasing step-by-step.

Here, according to the hypothesis and illustration above, the volume, as a function of time, can be written as:

$$V(t) = V_0 + \Delta V(t) = [l_{pa} + \Delta l_{pa}(t)] \times [l_{pa} + \Delta l_{pa}(t)] \times [l_{pe} + \Delta l_{pe}(t)] \quad (1)$$

$$l_{pa} = l_{pe}, \Delta l_{pa}(t) = \Delta l_{pe}(t) \quad (2)$$

At adsorption time t, the swelling of coal as a function of time is:

$$Q(t) = \frac{V(t) - V_0}{V_0} \quad (3)$$

The swelling before ith adsorption is $Q(t)_{i-1}$ (the swelling at the end of time exposure to P_{i-1}). At the ith adsorption pressure step, $Q(t)_i$ is the swelling at the end of time exposure to P_i. The fractional swelling increment is $q_i(t)$ during the coal sample is exposed to P_i [45]:

$$q_i(t) = \frac{\frac{V(t)-V_0}{V_0} - Q_{i-1}}{Q_i - Q_{i-1}} \quad (4)$$

where $q_i(t)$ is the volume strain change of the ith pressure step, which ranges from 0 to 1. $q_i(t) = 0$ means that adsorption just recently occurs at the P_i pressure step, and the swelling increment instantaneously changes with the adsorption amount. $q_i(t) = 1$ indicates that the swelling has reached equilibrium at the given gas pressure P_i. In order to facilitate the use of the elastic mechanic theory, Equation (4) is converted to the form as follows:

$$q_i(t) = \Delta\varepsilon_{vi}(t) \quad (5)$$

Here, the $\Delta\varepsilon_{vi}(t)$ means the fractional volumetric swelling increment from P_{i-1} to P_i.

Except for swelling, the given adsorption pressure generates volume compression due to closure of fractures and cleats, and coal matrix solid is also compressed during the loading process. In this process, the elastic modulus and Poisson's ratio are not fixed values. Goodman [46] suggested that the strain variation by pressure independent action was:

$$\varepsilon_P = -\frac{P}{E_s}(1 - 2\nu_s) \tag{6}$$

Exposure to the given P_i pressure step, the fractional strain variation of the sample is $\Delta\varepsilon_{Pi}$ from P_{i-1} to P_i

$$\Delta\varepsilon_{P_i} = -\frac{\Delta P_i}{E_s}(1 - 2\nu_s) \tag{7}$$

where ΔP_i is the pressure increment from P_{i-1} to P_i. E_s is the elastic modulus of coal matrix solid, which is not equivalent to the Young's modulus (E_P) that takes the elasticity of micropores into account. The relationship between the elastic modulus E_s and the Young's modulus E_P can be expressed as [47]:

$$E_s = \frac{E_P(3\rho_s - 2\rho)}{\rho} \tag{8}$$

ρ_s and ρ are the density of the solid phase (skeletal density) and apparent density, respectively.

According to Bentz et al. [48], Poisson' ratio change can be expressed in Equation (9) after sorption

$$\nu = \nu_s + \frac{3(1 - \nu_s^2)(1 - 5\nu_s)\phi}{2(7 - 5\nu_s)} \tag{9}$$

where ν_s is the Poisson ratio of the solid frame, ranging from -1 to 0.5, ν is the effective Poisson ratio, and ϕ is the porosity. In the process of deduction, it was assumed that the pore shape was cylindrical and the pores were randomly distributed. The relationships of $E_P/E_s - \rho/\rho_s$ as well as $\nu - \nu_s$ based on the research data of Bentz et al. [48] are shown in Figure 4.

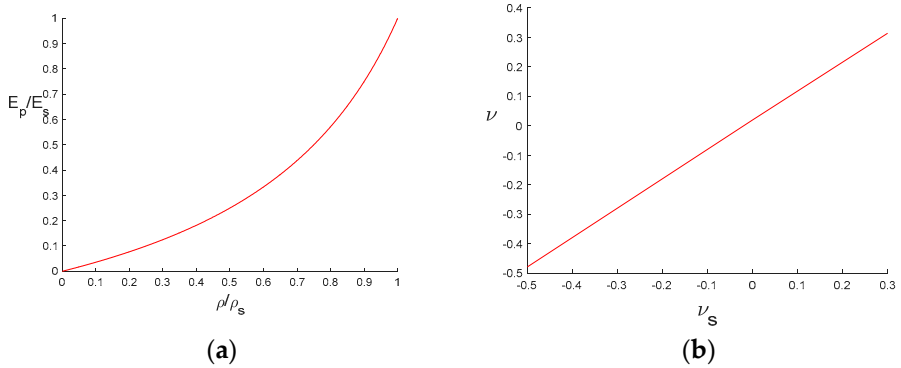

Figure 4. (**a**) The relationship of E_P/E_s and ρ/ρ_s; (**b**) the linear figure of ν against ν_s (ϕ = 0.07) [48].

The fractional volumetric strain increment and the total volumetric strain is $\Delta\varepsilon_i$ and ε_i, respectively. Two parts are included, gas adsorption induced matrix swelling strain $\Delta\varepsilon_{vi}$, taken as positive, and adsorption pressure loading induced strain $\Delta\varepsilon_{Pi}$, taken as negative:

$$\Delta\varepsilon_i = \Delta\varepsilon_{vi} - \Delta\varepsilon_{Pi} \tag{10}$$

$$\varepsilon_i(t) = \sum_{i=1}^{n}(\Delta\varepsilon_{vi} - \Delta\varepsilon_{Pi}) = \sum_{i=1}^{n}\left[\frac{\frac{V(t)-V_0}{V_0} - Q_{i-1}}{Q_i - Q_{i-1}} + \frac{\Delta P_i}{E_s}(1 - 2\nu_s)\right] \tag{11}$$

Equation (11) is an expression of the total volumetric strain after equilibrium by pressure increasing step-by-step under unconfined conditions. This expression of adsorption-induced volumetric swelling strain considers the initial volume V_0 and the volume at the time of t. In addition, the changes of Young's modulus and Poisson ratio are also contained.

Under the hypothesis of isotropic and homogeneous, based on the relationship between linear strain and volumetric strain in elastic mechanics, and the linear swelling strain in the vertical direction can be expressed as follows:

$$\varepsilon_{iz}(t) = \frac{1}{3}\varepsilon_i(t) = \frac{1}{3}\sum_{i=1}^{n}\left[\frac{\frac{V(t)-V_0}{V_0} - Q_{i-1}}{Q_i - Q_{i-1}} + \frac{\Delta P_i}{E_s}(1-2\nu_s)\right] \tag{12}$$

2.2. Adsorption-Induced Stress under Uniaxial Conditions

After the mining work finished, only two parts of pillars and goafs are left in the original work face (Figure 5). Due to the overburden pressure and stress redistribution by mining activities, the pillar bears the pressure of overlying strata as well as mining stress and preforms uniaxial condition (Figure 6). If the CO_2 gas (fluid) is injected in goaf, this adsorption behavior will occur in the pillar. Under the uniaxial condition, adsorption-induced swelling strain occurs on the two sides adjacent to goafs and drifts, but the swelling strain of the direction perpendicular to bedding is inhibited, resulting in the swelling stress occurring in the vertical direction (z axial, Figure 3). The swelling stress can decrease crack initiation stress, resulting in the damage of the coal pillar. In this section, we consider the derivation of swelling stress in the direction perpendicular to bedding.

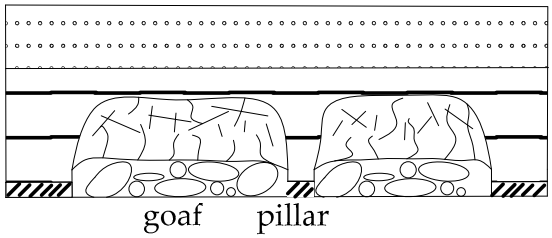

Figure 5. Schematic diagram of pillar and goaf in the abandoned coal mine.

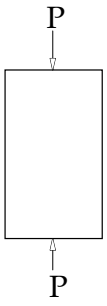

Figure 6. Schematic diagram of the uniaxial condition of the pillar.

Based on the analysis of the section above, under uniaxial conditions, the constitutive relation of swelling stress and swelling strain in the vertical direction (z axial) follows Equation (13):

$$\sigma_{iz} = E_s\varepsilon_{iz} \tag{13}$$

Combining Equations (12)–(14), stress increment in the vertical direction in the process of exposure from P_{i-1} to P_i can be calculated by Formula (15). The swelling stress includes two parts. The first part is the adsorption-induced swelling stress, and the second is volume-compressed stress:

$$\Delta\varepsilon_{iz}(t) = \frac{1}{3}\Delta\varepsilon_i(t) \tag{14}$$

$$\Delta\sigma_{iz}(t) = E_s\Delta\varepsilon_{iz}(t) = \frac{E_s}{3}[\frac{\frac{V(t)-V_0}{V_0} - Q_{i-1}}{Q_i - Q_{i-1}} + \frac{\Delta P_i}{E_s}(1-2\nu_s)] \tag{15}$$

If, at the given nth pressure step, P_n, the pillar perfectly reaches adsorption equilibrium, and the fractional swelling variation does not change and the linear strain also remains constant. In this case, the swelling stress is the cumulative value of stress increments at overall adsorption pressure steps:

$$\sigma_{iz}(t) = \sum_{i=1}^{n}\Delta\sigma_{iz}(t) = \sum_{i=1}^{n}\frac{E_s}{3}[\frac{\frac{V(t)-V_0}{V_0} - Q_{i-1}}{Q_i - Q_{i-1}} + \frac{\Delta P_i}{E_s}(1-2\nu_s)] \tag{16}$$

where $\sigma_{iz}(t)$ is the total swelling stress considering the adsorption occurring in the pillar in the vertical direction where swelling strain is inhibited under the uniaxial condition. The swelling stress is a cumulative value by step-by-step pressures loading from 1st to nth steps.

2.3. Mechanical Strength Change after Gas Adsorption

The pillar coal matrix swells after CO_2 injection in abandoned coal mines, while it shrinks when gas is expelled from coal mass. Adsorption expansion will inevitably lead to some changes in the mechanical properties of the pillar, such as the above mentioned parameters, elastic modulus, Poisson's ratio, bulk modulus as well as shear modulus, due to these parameters being highly effected by adsorption-induced fracturing. All of these variations result in the decrease of pillar strength during CO_2 sequestration in abandoned coal mines. Hu et al. [49] demonstrated that the adsorption of gas exhibits dual effects on the physical properties of coal, mechanical (swelling stress) and non-mechanical (erosion effect) effects. The swelling effect leads to the decrease of the interaction between coal particles, while the erosion effect reduces the surface energy and lowers the surface tension of the coal mass. Gas adsorption mainly affects the cohesion, and the decrease of cohesion leads to obvious plastic deformation of coal, but, for the internal friction angle, it decreases to a certain extent and the hold over no longer changes. Hol et al. [40] verified that gas sorption can lead to a decrease in bulk modulus, while an increase in swelling caused the strain hysteresis to be oversized during the process of loading–unloading. Hagin and Zoback [50] compared the adsorption characteristics of CO_2 with that of helium, and found that the Young's modulus decreased after the CO_2 saturation adsorption. Simultaneously, the static bulk modulus reduced by an order of magnitude. Yang and Zoback [51] observed that CO_2 injection into coal samples resulted in the volume increase, and the coal sample became more viscous and less elastic. Ranjith and Perera [41] considered the effects of cleat density and direction on CO_2 adsorption-induced strength reduction.

On the basis of Griffith line elastic fracture theory, when cracks propagate, a portion of the elastic energy is converted into a solid surface energy. The fracture is confined in the extended critical state when the release rate of the elastic energy is equal to the increase rate of the surface energy. In the plane stress state, the critical stress is:

$$\sigma_c = \sqrt{\frac{2E\gamma}{\pi a}} \tag{17}$$

where γ is the surface energy per unit area, N/m; π is the surface tension change value from the vacuum to the given adsorption condition, N/m. In the case of the plane strain state, E is replaced by

$E-(1-\upsilon^2)$. Furthermore, the relationship between the solid linear expansion strain and the change in surface tension is as follows:

$$\varepsilon = \lambda\pi = \lambda(\gamma_0 - \gamma_s) \tag{18}$$

where γ_0 and γ_s are the vacuum state and surface tension after gas adsorption, respectively, and λ can be described as Equation (19) [52]:

$$\lambda = \frac{2S\rho}{9K_s} \tag{19}$$

$$K_s = \frac{E_s}{3(1-2\nu_s)} \tag{20}$$

where S is the specific surface area of the coal sample, and K_s is the apparent modulus.

Equation (18) is rewritten as:

$$\gamma_s = \gamma_0 - \frac{\varepsilon_{iz}}{\lambda} \tag{21}$$

By Equation (17), the critical propagation stress at the end of the given pressure P_n for the nth adsorption step is expressed as function of time and swelling stress:

$$\sigma_{ci}(t) = \sqrt{\frac{2E_s(\gamma_0 - \frac{\varepsilon_{iz}(t)}{\lambda})}{\pi a}} = \sqrt{\frac{2E_s(\gamma_0 - \frac{\sum_{i=1}^{n}\Delta\sigma_{iz}(t)}{E_s\lambda})}{\pi a}} \tag{22}$$

It can be written as:

$$\sigma_{ci}^2(t) = \frac{2E_s\gamma_0}{\pi a} - \frac{2\sum_{i=1}^{n}\Delta\sigma_{iz}(t)}{\lambda\pi a} \tag{23}$$

The square of the critical strength in vacuum conditions is σ_{c0}^2, as the following

$$\sigma_{c0}^2 = \frac{2E_s\gamma_0}{\pi a} \tag{24}$$

At the end of exposure to the nth adsorption pressure step, the strength reduction rate of the pillar is the ratio of $\sigma_{ci}^2(t)$ to σ_{c0}^2

$$\left(\frac{\sigma_{ci}(t)}{\sigma_{c0}}\right)^2 = 1 - \frac{\sum_{i=1}^{n}\Delta\sigma_{iz}(t)}{E_s\lambda\gamma_0} \tag{25}$$

That is,

$$\left(\frac{\sigma_{ci}(t)}{\sigma_{c0}}\right)^2 = 1 - \frac{E_s\sum_{i=1}^{n}\left[\frac{\frac{V(t)-V_0}{V_0} - Q_{i-1}}{Q_i - Q_{i-1}} + \frac{\Delta P_i}{E_s}(1-2\nu_s)\right]}{2S\rho\gamma_0(1-2\nu_s)} \tag{26}$$

Equation (26) is the calculation formula of the strength reduction rate considering the swelling stress increment under the condition of gas adsorption at partial pressure loading step-by-step. The formula can be used to calculate the strength reduction value of gas adsorption conveniently. The curve of ratio $\sigma_{ci}^2(t)$ to σ_{c0}^2 is showed in Figure 7, and the strength reduction is nearly 17% after adsorption equilibrated based on the swelling strain data at pressure 2 MPa from [45]. Compared with other formulas of linear pressure adsorption models, Equation (14) is a progressive accumulation form that could be applied to calculate the swelling stress of nonlinear adsorption pressure loading–unloading. Moreover, in the case of re-adsorption after the coal sample having already swelled to a certain degree, Equations (16) and (26) are also helpful for determining the swelling stress fractional increment and strength reduction value.

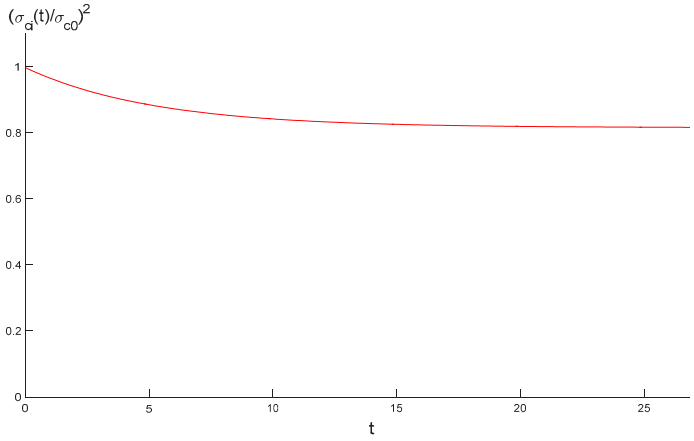

Figure 7. The reduction ratio curve of adsorption strength ($\sigma^2_{ci}(t)$) to original strength (σ^2_{c0}) over time. The swelling strain data are collected from [45].

3. Discussion

3.1. Swelling Strain and Swelling Stress

In this paper, we consider the volumetric swelling strain $\varepsilon_i(t)$ and isotropic linear strain ($\varepsilon_{iz}(t)$) in the z axial direction (Figure 3) as function of time after equilibrium by adsorption pressure increasing step-by-step under unconfined conditions. In connection with swelling strain, Hol et al. [38] and Liu et al. [39] considered thermodynamic models of gas adsorption and studied the effect of stress on the adsorption concentration of gas as well as sorption behavior. Their starting point is different from this paper based on directly volumetric changes. In the paper of Liu et al. [39], they established the relationship of internal energy, chemical potential, entropy change as well as stress–strain work on a single molecule of gas absorbed by the coal matrix cube. The strain was divided into mean extensional strain and deviatoric strain. In the deviation process of volumetric strain in this paper, it is easy to measure the strain increment without considering the thermodynamic process of adsorption. However, the coupling based on thermodynamic between stress–strain-sorption is significant important to understand the effect of pressure and temperature on adsorption in coal matrix. The swelling strain was divided into a reversible part and irreversible part under unconfined conditions [53]. Similarly, Wang et al. [54] divided strain into two parts at an isothermal condition. One is the mechanical deformation meeting the Hooke law stress–strain relationship and is calculated by the effective stress. The other is the deformation induced by gas adsorption or desorption. In Section 2, we do not mention it because not only an elastic strain but also an irreversible strain are converted to swelling stress considered from a macro perspective in the vertical direction under uniaxial loading.

In addition, based on the energy conservation law, and from the viewpoint of surface tension change, Wu et al. [55] and Bai et al. [56] utilized the principle that the expansion of the strain energy equals the surface tension work in order to establish the constitutive equation of swelling stress and swelling strain. Some researchers held the view that gas adsorption satisfies the Langmuir isothermal adsorption model (Figure 8), and considers the linear relationship between adsorption capacity and swelling strain. Although a large number of studies have shown that gas adsorption presents a single molecule arrangement structure that meets the Langmuir model, Lin [57] and Yu et al. [58] suggested that CO_2 adsorption on the coal mass can be described in a multi adsorbed layer model, i.e., the Brunauer-Emmett-Teller (BET) adsorption type model.

Langmuir isotherm adsorption model equation is given by:

$$q = \frac{abp_{\mathrm{p}}}{1 + bp_{\mathrm{p}}} \tag{27}$$

where q is the adsorbed amount of gas during adsorption reaching equilibrium, a is the gas limit adsorption capacity at the reference pressure, b is the adsorption equilibrium constant, and p_p is the pore pressure.

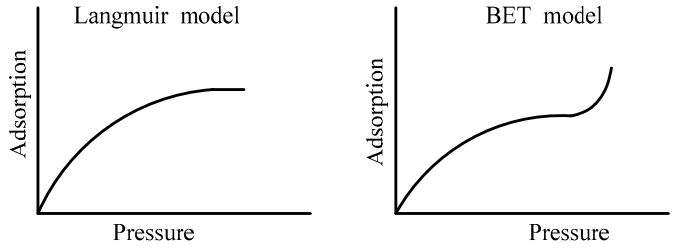

Figure 8. Two types of adsorption isotherms.

In the study of the acid gas CO_2 and H_2S storage in coal seam, Chikatamarla et al. [59] also calculated the frictional expansion strain by the Langmuir model:

$$V = \frac{V_L P}{P_L + P} \tag{28}$$

$$\varepsilon_V = \frac{\varepsilon_L p}{p + p_e} \tag{29}$$

where V, P, V_L, P_L are gas adsorption volume, adsorption pressure, Langmuir volume and Langmuir pressure, respectively. In addition, ε_V and ε_L are, respectively, the strain at given pressure and strain at infinite pressure, and p_e is the Langmuir pressure constant, which is equal to the pressure value when the strain at the pressure is half of the Langmuir maximum strain.

For the cylindrical specimen, according to the isotropic assumption of swelling/collapse in the process of adsorption/desorption, the volume strain is expressed as:

$$\varepsilon = \frac{\Delta V}{V} = \varepsilon_r^2 + 2\varepsilon_r + \varepsilon_a + \varepsilon_r^2 \varepsilon_a + 2\varepsilon_a \varepsilon_r \tag{30}$$

where V and ΔV are the initial volume and the volume change, respectively. ε_a and ε_r are, respectively, the axial strain and the radial strain.

Robertson and Christiansen [60] introduced the strain factor function to modify the Langmuir strain constant. The strain factor function is given by

$$s_f = \frac{p_{ob}}{p}[a + b(\frac{P_L}{\varepsilon_L V_r^2 \sqrt{\gamma}})] \tag{31}$$

where p_{ob} denotes the overburden pressure, a and b are empirical constants, V_r denotes the vitrinite reflectance of coal, and γ denotes the bulk density of the gas. p, ε_L and P_L are consistent with Equations (28) and (29).

The BET adsorption model is a generalization of the Langmuir model considering multi adsorbed molecule layers, which is expressed by [57,61]

$$q = \frac{V_m C P}{(P_0 - P)[1 + (C-1)P/P_0]} \tag{32}$$

where P_0 is the saturation pressure of gas, P is the adsorption pressure, V_m is the maximum adsorption volume at the time the entire adsorbent surface is covered with a complete single molecular layer, and C is a constant related to the net heat of adsorption.

On the basis of the isotropic assumption and the Langmuir adsorption model, the above mentioned literature obtained the stress–strain relationship of swelling. All of those models follow

a certain degree of representation in accordance with adsorption induced-swelling. However, they are not perfect because the Langmuir model has a very high accuracy and precision in the case of describing low-pressure gas adsorption. However, it is not suitable for high temperature gas adsorption, particularly, when CO_2 is sequestrated in deep unmined coal seams, where it is confined in states of high temperature and high pressure. Under the situation that CO_2 may exhibit a supercritical state that includes dual characteristics of gas and liquid, and the density of supercritical CO_2 fluid is close to that of the liquid, but the viscosity of which is similar to that of the gas. The diffusion coefficient of supercritical CO_2 is nearly one hundred times of that of the liquid.

Although this paper is also based on the isotropic hypothesis to establish the stress–strain relationship as a function of time and each adsorption pressure step, we do not consider the Langmuir isothermal adsorption model as the reference model but directly analyze it based on volume increment. Furthermore, other models only consider the initial state and the final equilibrium state and have exclusively been expressed in single integral steps, whilst the swelling increment of the prior swelled sample under re-loading is not taken into account.

3.2. Stress and Strength Reduction

Coupling relationship of swelling strains, swelling stressed and total gas uptake are affected by coal properties. Fractured coal possesses dual porosity system: (a) the cleat macroporosity system, and (b) the microporosity of coal matrix. Espinoza et al. [62,63] proposed a double porosity poromechanical model and considered the strains as a function of stresses, fracture pore pressure, and the pressure-dependent adsorption stress developed by the coal matrix.

Liu et al. [64] considered the seepage model of fracture–matrix interaction during coal deformation, and put forward the concept of internal swelling stress, σ_I (Figure 9). The strain is considered including two parts: the first part is the coal matrix strain induced by the internal swelling stress, and the second part is the volume strain of the fracture. Their work modified the form of effective stress, so that the corrected expression of effective stress can directly reflect its impact on the permeability. Nevertheless, the elastic modulus, Poisson's ratio as well as other parameters are variable rather than fixed values during the occurrence of coal matrix adsorption swelling. These variates are not taken into account in the derivation of theory and formula, which leads to some errors in the accuracy of the model.

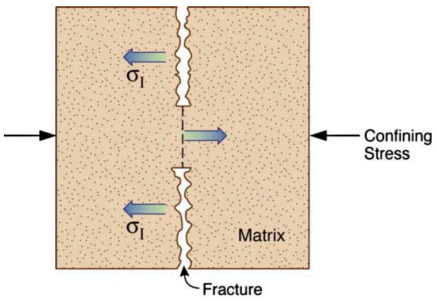

Figure 9. Graphical description of the internal swelling stress ([64]).

However, desorption differs from adsorption. Gas desorption can induce coal matrix shrinkage and stress relaxation. Espinoza et al. [65] studied the desorption-induced shear failure under zero-lateral strain condition and simulated the stress path far from the wellbore. Pore pressure in the coal cleats and desorption-induced variations of stresses jointly affect the stress path, i.e., poroelastic coefficient and variation changes of fluid pressure, as well as lateral stress decrease by desorption. The two part change effective stress of coal results in the stress path reaching the failure envelope. Wang et al. [66] considered gas desorption weakens coal by reducing effective stress. Desorption-induced shrinkages can relax lateral stress and aggravate shear failure of coal.

Ranjith et al. [32] considered CO_2 adsorption and mechanical behavior of coal, and held that peak strength could decrease when coal is saturated with CO_2. However, they did not comprehensively interpret the strength reduction mechanism. In this research, pillars are assumed to reach equilibrium on both sides of goaf after the mining working finished, and pillars are under the uniaxial condition. The coal pillar strength reduction is theoretically analyzed, and adsorption can increase the swelling stress on the faces of microfractures and cleats, resulting in effective stress decreasing. Under the condition of uniaxial conditions, if the loading pressure remains constant, and no swelling occurs, cracks could maintain the equilibrium state. However, when adsorption behaviors take place, the crack surface tension changes, and swelling stress emerges by swelling strain being inhibited. The stress needed to cause crack initiation is decreased, leading to coal pillars potentially being more prone to failure. The model proposed in this paper can describe the effect of swelling stress on strength clearly.

Coal is a solid that contains a large number of slit-like pores and fractures inter-connected by narrow capillary constriction and connected to the surface [67], which presents absolutely anisotropy and heterogeneity. Simultaneously, the adsorption induced-swelling also has anisotropic characteristics for the reason that most microfractures developed parallel to the bedding plate, approximately following maceral–maceral and bedding interfaces and swelling anisotropic [53]. In this paper, it is assumed that both coal and swelling have isotropic elastic properties for conveniently facilitating the application of existing theories and simplifying the process of calculation. From the perspective of CO_2 sequestration in abandoned coal mines, the strength change of coal pillars must be emphasized to prevent CO_2 leakage from goafs. To accurately predict the swelling stress in the vertical direction and strength reduction of pillars, much more research and many more approaches are still required.

4. Conclusions

This study has focused on volumetric swelling strain and strength reduction of pillars when CO_2 is stored in abandoned coal mines. The volumetric swelling strain is theoretically derived as a function of time by adsorption pressure increasing step-by-step under unconfined conditions. In connection with the conditions of coal pillars in abandoned coal mines, and a uniaxial loading model is proposed by simplifying the actual condition. Swelling strain in a direction perpendicular to bedding is inhibited when CO_2 adsorption is in the pillar. The effect of adsorption on pillar strength reduction is theoretically analyzed and deduced. Our findings can be summarized as follows:

1. There are a large number of coal mines that will be closed and some of them are located in deep formations in China. CO_2 storage in abandoned coal mines could be a potential option for greenhouse gas disposal.
2. The volume strain and swelling stress, as a function of time, and different loading pressure steps are deduced. Equation (15) is used to describe swelling stress considering coal has already had prior swelling deformation under the condition of step-by-step non-linear loading and a non-Langmuir isothermal model. The model presented in this paper is different from other models, in which only the initial state and the final equilibrium state are considered, and the incremental swelling process is neglected.
3. A theoretical model based on linear swelling stress–strain work is proposed to calculate the reduction ratio of coal pillar strength under uniaxial conditions. This theoretical model can be used to describe strength reduction during adsorption under adsorption pressure loading step-by-step.

Acknowledgments: The National Basic Research Program of China (Grant No. 2011CB013500), the National Key Research and Development Plan (Grant No. 2016YFC0501104), the National Natural Science Foundation of China (Grant No. U1361103, 51479094, 51379104), the National Natural Science Foundation Outstanding Youth Foundation (Grant No. 51522903), and the Open Research Fund Program of the State Key Laboratory of Hydroscience and Engineering (Grant 2013-KY-06, 2015-KY-04, 2016-KY-02) are gratefully acknowledged.

Author Contributions: Xiaoli Liu designed the research; Qiuhao Du performed the research; Enzhi Wang and Sijing Wang contributed reagents/materials/analysis tools; and Qiuhao Du wrote the paper. All authors read and approved the manuscript.

Conflicts of Interest: The authors declare no conflict of interest.

References

1. Zhang, F.; Zhou, H.; Lu, T.; Hu, D.W.; Sheng, Q.; Hu, Q.Z. Analysis of reservoir deformation and fluid transportation induced by injection of CO_2 into saline aquifer: (I) Two-phase flow-reservoir coupling model. *Rock Soil Mech.* **2014**, *35*, 2549–2554. (In Chinese)
2. Edenhofer, O. Mitigation of climate change IA models and WGIII: Lessons from IPCC AR5. In Proceedings of the 7th IAMC Meeting, Valencia, Spain, 23–25 October 2014.
3. International Energy Agency (IEA). *Four Energy Policies Can Keep the 2 °C Climate Goal Alive*; International Energy Agency (IEA): Paris, France, 2013.
4. Seomoon, H.; Lee, M.; Sung, W. Analysis of methane recovery through CO_2-N_2 mixed gas injection considering gas diffusion phenomenon in coal seam. *Energy Explor. Exploit.* **2016**, *34*, 661–675. [CrossRef]
5. He, L.; Shen, P.; Liao, X.; Li, F.; Gao, Q.; Wang, Z. Potential evaluation of CO_2 EOR and sequestration in Yanchang oilfield. *J. Energy Inst.* **2016**, *89*, 215–221. [CrossRef]
6. Chareonsuppanimit, P.; Mohammad, S.A.; Robinson, R.L.; Gasem, K.A.M. High-pressure adsorption of gases on shales: Measurements and modeling. *Int. J. Coal Geol.* **2012**, *95*, 34–46. [CrossRef]
7. Lu, Y.; Ao, X.; Tang, J.; Jia, Y.; Zhang, X.; Chen, Y. Swelling of shale in supercritical carbon dioxide. *J. Nat. Gas Sci. Eng.* **2016**, *30*, 268–275. [CrossRef]
8. Day, S.; Fry, R.; Sakurovs, R.; Weir, S. Swelling of coals by supercritical gases and its relationship to sorption. *Energy Fuels* **2010**, *24*, 2777–2783. [CrossRef]
9. Piessens, K.; Dusar, M. Feasibility of CO_2 sequestration in abandoned coal mines in Belgium. *Geol. Belg.* **2004**, *7*, 168–180.
10. Piessens, K.; Dusar, M. Integration of CO_2 sequestration and CO_2 geothermics in energy systems for abandoned coal mines. *Geol. Belg.* **2004**, *7*, 181–189.
11. Van Tongeren, P.; Dreesen, R. Residual space volumes in abandoned coal mines of the Belgian Campine basin and possibilities for use. *Geol. Belg.* **2004**, *7*, 157–164.
12. Jalili, P.; Saydam, S.; Cinar, Y. CO_2 storage in abandoned coal mines. In Proceedings of the 2011 Underground Coal Operators' Conference, Beijing, China, 8–9 January 2011.
13. Van Krevelen, D.W. *Coal-Typology, Chemistry, Physics, Constitution*; Elsevier: Amsterdam, The Netherlands, 1961.
14. Sanada, Y.; Honda, H. Swelling equilibrium of coal by pyridine at 25 degrees C. *Fuel* **1966**, *45*, 295.
15. Solomon, P.R.; Fletcher, T.H. Impact of coal pyrolysis on combustion. *Symp. (Int.) Combust.* **1994**, *25*, 463–474.
16. Walker, P.L.; Verma, S.K.; Rivera-Utrilla, J.; Khan, M.R. A direct measurement of expansion in coals and macerais induced by carbon dioxide and methanol. *Fuel* **1988**, *67*, 719–726. [CrossRef]
17. Karacan, C.Ö. Swelling-induced volumetric strains internal to a stressed coal associated with CO_2 sorption. *Int. J. Coal Geol.* **2007**, *72*, 209–220. [CrossRef]
18. Pan, Z.; Connell, L.D. Modelling of anisotropic coal swelling and its impact on permeability behaviour for primary and enhanced coalbed methane recovery. *Int. J. Coal Geol.* **2011**, *85*, 257–267. [CrossRef]
19. Feng, Z.; Zhou, D.; Zhao, Y.; Cai, T. Study on microstructural changes of coal after methane adsorption. *J. Nat. Gas Sci. Eng.* **2016**, *30*, 28–37. [CrossRef]
20. Shovkun, I.; Espinoza, D.N.; Ramos, M.J. Coupled reservoir simulation of geomechanics and fluid flow in organic-rich rocks: Impact of gas desorption and stress changes on permeability during depletion. In Proceedings of the 50th US Rock Mechanics/Geomechanics Symposium, Houston, TE, USA, 26–29 June 2016.
21. Heller, R.; Zoback, M. Adsorption of methane and carbon dioxide on gas shale and pure mineral samples. *J. Unconv. Oil Gas Resour.* **2014**, *8*, 14–24. [CrossRef]
22. Hol, S.; Spiers, C.J. Competition between adsorption-induced swelling and elastic compression of coal at CO_2 pressures up to 100 MPa. *J. Mech. Phys. Solids* **2012**, *60*, 1862–1882. [CrossRef]
23. Zang, J.; Wang, K. Gas sorption-induced coal swelling kinetics and its effects on coal permeability evolution: Model development and analysis. *Fuel* **2017**, *189*, 164–177. [CrossRef]

24. Feng, R.; Harpalani, S.; Pandey, R. Laboratory measurement of stress-dependent coal permeability using pulse-decay technique and flow modeling with gas depletion. *Fuel* **2016**, *177*, 76–86. [CrossRef]
25. Connell, L.D. A new interpretation of the response of coal permeability to changes in pore pressure, stress and matrix shrinkage. *Int. J. Coal Geol.* **2016**, *162*, 169–182. [CrossRef]
26. Zhang, L.; Zhang, C.; Tu, S.; Tu, H.; Wang, C. A study of directional permeability and gas injection to flush coal seam gas testing apparatus and method. *Transp. Porous Media* **2016**, *111*, 573–589. [CrossRef]
27. Connell, L.D.; Mazumder, S.; Sander, R.; Camilleri, M.; Pan, Z.; Heryanto, D. Laboratory characterisation of coal matrix shrinkage, cleat compressibility and the geomechanical properties determining reservoir permeability. *Fuel* **2016**, *165*, 499–512. [CrossRef]
28. Peng, Y.; Liu, J.; Pan, Z.; Connell, L.D.; Chen, Z.; Qu, H. Impact of coal matrix strains on the evolution of permeability. *Fuel* **2017**, *189*, 270–283. [CrossRef]
29. Jasinge, D.; Ranjith, P.G.; Choi, X.; Fernando, J. Investigation of the influence of coal swelling on permeability characteristics using natural brown coal and reconstituted brown coal specimens. *Energy* **2012**, *39*, 303–309. [CrossRef]
30. Ranjith, P.G.; Perera, M.S.A. A new triaxial apparatus to study the mechanical and fluid flow aspects of carbon dioxide sequestration in geological formations. *Fuel* **2011**, *90*, 2751–2759. [CrossRef]
31. Verma, A.K.; Sirvaiya, A. Comparative analysis of intelligent models for prediction of Langmuir constants for CO_2 adsorption of Gondwana coals in India. *Geomech. Geophys. Geo Energy Geo Resour.* **2016**, *2*, 97–109. [CrossRef]
32. Ranjith, P.G.; Jasinge, D.; Choi, S.K.; Mehic, M.; Shannon, B. The effect of CO_2 saturation on mechanical properties of Australian black coal using acoustic emission. *Fuel* **2010**, *89*, 2110–2117. [CrossRef]
33. Viete, D.R.; Ranjith, P.G. The mechanical behaviour of coal with respect to CO_2 sequestration in deep coal seams. *Fuel* **2007**, *86*, 2667–2671. [CrossRef]
34. Vishal, V.; Ranjith, P.G.; Singh, T.N. An experimental investigation on behaviour of coal under fluid saturation, using acoustic emission. *J. Nat. Gas Sci. Eng.* **2015**, *22*, 428–436. [CrossRef]
35. Myers, A.L. Thermodynamics of adsorption in porous materials. *AIChE J.* **2002**, *48*, 145–160. [CrossRef]
36. Myers, A.L.; Monson, P.A. Adsorption in porous materials at high pressure: Theory and experiment. *Langmuir* **2002**, *18*, 10261–10273. [CrossRef]
37. Pan, Z.; Connell, L.D. A theoretical model for gas adsorption-induced coal swelling. *Int. J. Coal Geol.* **2007**, *69*, 243–252. [CrossRef]
38. Hol, S.; Peach, C.J.; Spiers, C.J. Effect of 3-D stress state on adsorption of CO_2 by coal. *Int. J. Coal Geol.* **2012**, *93*, 1–15. [CrossRef]
39. Liu, J.; Spiers, C.J.; Peach, C.J.; Vidal-Gilbert, S. Effect of lithostatic stress on methane sorption by coal: Theory vs. experiment and implications for predicting in-situ coalbed methane content. *Int. J. Coal Geol.* **2016**, *167*, 48–64. [CrossRef]
40. Hol, S.; Gensterblum, Y.; Massarotto, P. Sorption and changes in bulk modulus of coal—Experimental evidence and governing mechanisms for CBM and ECBM applications. *Int. J. Coal Geol.* **2014**, *128*, 119–133. [CrossRef]
41. Ranjith, P.G.; Perera, M.S.A. Effects of cleat performance on strength reduction of coal in CO_2 sequestration. *Energy* **2012**, *45*, 1069–1075. [CrossRef]
42. Perera, M.S.A.; Ranjith, P.G.; Viete, D.R. Effects of gaseous and super-critical carbon dioxide saturation on the mechanical properties of bituminous coal from the Southern Sydney Basin. *Appl. Energy* **2013**, *110*, 73–81. [CrossRef]
43. Wang, S.; Hou, G.; Zhang, M.; Sun, Q. Analysis of the visible fracture system of coalseam in Chengzhuang Coalmine of Jincheng City, Shanxi Province. *Chin. Sci. Bull.* **2005**, *50*, 45–51. [CrossRef]
44. Liu, S.; Sang, S.; Liu, H.; Zhu, Q. Growth characteristics and genetic types of pores and fractures in a high-rank coal reservoir of the southern Qinshui basin. *Ore Geol. Rev.* **2015**, *64*, 140–151. [CrossRef]
45. Staib, G.; Sakurovs, R.; Gray, E.M.A. Kinetics of coal swelling in gases: Influence of gas pressure, gas type and coal type. *Int. J. Coal Geol.* **2014**, *132*, 117–122. [CrossRef]
46. Goodman, R.E. *Introduction to Rock Mechanics*; John Wiley & Sons: Hoboken, NY, USA, 1980.
47. Scherer, G.W. Dilatation of porous glass. *J. Am. Ceram. Soc.* **1986**, *69*, 473–480. [CrossRef]
48. Bentz, D.P.; Garboczi, E.J.; Quenard, D.A. Modelling drying shrinkage in reconstructed porous materials: Application to porous Vycor glass. *Model. Simul. Mater. Sci. Eng.* **1998**, *6*, 211. [CrossRef]

49. Hu, S.; Wang, E.; Li, X.; Bai, B. Effects of gas adsorption on mechanical properties and erosion mechanism of coal. *J. Nat. Gas Sci. Eng.* **2016**, *30*, 531–538. [CrossRef]
50. Hagin, P.N.; Zoback, M.D. Laboratory studies of the compressibility and permeability of low-rank coal samples from the Powder River Basin, Wyoming, USA. In Proceedings of the 44th US Rock Mechanics Symposium and 5th US-Canada Rock Mechanics Symposium, Salt Lake City, UT, USA, 27–30 June 2010.
51. Yang, Y.; Zoback, M.D. The effects of gas adsorption on swelling, visco-plastic creep and permeability of sub-bituminous coal. In Proceedings of the 45th U.S. Rock Mechanics/Geomechanics Symposium, San Francisco, CA, USA, 26–29 June 2011.
52. Adamson, A.W.; Gast, A.P. *Physical Chemistry of Surfaces*; Science Press: Beijing, China, 1984. (In Chinese)
53. Hol, S.; Spiers, C.J.; Peach, C.J. Microfracturing of coal due to interaction with CO_2 under unconfined conditions. *Fuel* **2012**, *97*, 569–584. [CrossRef]
54. Wang, G.X.; Massarotto, P.; Rudolph, V. An improved permeability model of coal for coalbed methane recovery and CO_2 geosequestration. *Int. J. Coal Geol.* **2009**, *77*, 127–136. [CrossRef]
55. Wu, S.Y.; Zhao, W. Analysis of effective stress in adsorbed methane-coal system. *Chin. J. Rock Mech. Eng.* **2005**, *24*, 1674–1678. (In Chinese)
56. Bai, B.; Li, X.C.; Liu, Y.F.; Fang, Z.M.; Wang, W. Preliminary theoretical study on impact on coal caused by interactions between CO_2 and coal. *Rock Soil Mech.* **2007**, *28*, 823–826. (In Chinese)
57. Lin, W. Gas Sorption and the Consequent Volumetric and Permeability Change of Coal. Ph.D. Thesis, Stanford University, Stanford, CA, USA, March 2010.
58. Yu, W.; Al-Shalabi, E.W.; Sepehrnoori, K. A sensitivity study of potential CO_2 injection for enhanced gas recovery in Barnett shale reservoirs. In Proceedings of the SPE Unconventional Resources Conference, The Woodlands, TX, USA, 1–3 April 2014.
59. Chikatamarla, L.; Cui, X.; Bustin, R.M. Implications of volumetric swelling/shrinkage of coal in sequestration of acid gases. In Proceedings of the International Coalbed Methane Symposium, Tuscaloosa, AL, USA, 3–7 May 2004.
60. Robertson, E.P.; Christiansen, R.L. Modeling laboratory permeability in coal using sorption-induced strain data. *SPE Reserv. Eval. Eng.* **2007**, *10*, 260–269. [CrossRef]
61. Sing, K.S.W. Reporting physisorption data for gas/solid systems with special reference to the determination of surface area and porosity (Recommendations 1984). *Pure Appl. Chem.* **1985**, *57*, 603–619. [CrossRef]
62. Espinoza, D.N.; Vandamme, M.; Pereira, J.M.; Dangla, P.; Vidal-Gilbert, S. Measurement and modeling of adsorptive-poromechanical properties of bituminous coal cores exposed to CO_2: Adsorption, swelling strains, swelling stresses and impact on fracture permeability. *Int. J. Coal Geol.* **2014**, *134*, 80–95. [CrossRef]
63. Espinoza, D.N.; Vandamme, M.; Dangla, P.; Pereira, J.M.; Vidal-Gilbert, S. Adsorptive-mechanical properties of reconstituted granular coal: Experimental characterization and poromechanical modeling. *Int. J. Coal Geol.* **2016**, *162*, 158–168. [CrossRef]
64. Liu, H.H.; Rutqvist, J. A new coal-permeability model: Internal swelling stress and fracture-matrix interaction. *Transp. Porous Media* **2010**, *82*, 157–171. [CrossRef]
65. Espinoza, D.N.; Pereira, J.M.; Vandamme, M.; Dangla, P.; Vidal-Gilbert, S. Desorption-induced shear failure of coal bed seams during gas depletion. *Int. J. Coal Geol.* **2015**, *137*, 142–151. [CrossRef]
66. Wang, S.; Elsworth, D.; Liu, J. Permeability evolution during progressive deformation of intact coal and implications for instability in underground coal seams. *Int. J. Rock Mech. Min. Sci.* **2013**, *58*, 34–45. [CrossRef]
67. Melnichenko, Y.B.; He, L.; Sakurovs, R.; Kholodenko, A.L.; Blach, T.; Mastalerz, M.; Andrzej, P.; Radliński, A.; Cheng, G.; Mildner, D.F.R. Accessibility of pores in coal to methane and carbon dioxide. *Fuel* **2012**, *91*, 200–208. [CrossRef]